Contents lists available at ScienceDirect

ISPRS Journal of Photogrammetry and Remote Sensing

Assessing local climate zones in arid cities: The case of Phoenix, Arizona and Las Vegas, Nevada

Chuyuan Wang [a], Ariane Middel [b,*], Soe W. Myint [a], Shai Kaplan [c], Anthony J. Brazel [a], Jonas Lukasczyk [d]

[a] *School of Geographical Sciences and Urban Planning, Arizona State University, Tempe, AZ 85287, USA*
[b] *Department of Geography and Urban Studies, Temple University, Philadelphia, PA 19122, USA*
[c] *Ben-Gurion University of the Negev, Beer-Sheva, Israel*
[d] *Department of Computer Science, University of Kaiserslautern, Kaiserslautern 67663, Germany*

ABSTRACT

The local climate zone (LCZ) classification scheme is a standardization framework to describe the form and function of cities for urban heat island (UHI) studies. This study classifies and evaluates LCZs for two arid desert cities in the Southwestern United States – Phoenix and Las Vegas – following the World Urban Database and Access Portal Tools (WUDAPT) method. Both cities are classified into seven built type LCZs and seven land-cover type LCZs at 100-m resolution using Google Earth, Saga GIS, and Landsat 8 scenes. Average surface cover properties (building fraction, impervious fraction, pervious fraction) and sky view factors of classified LCZs are then evaluated and compared to pre-defined LCZ representative ranges from the literature, and their implications on the surface UHI (SUHI) effect are explained. Results suggest that observed LCZ properties in arid desert environments do not always match the proposed value ranges from the literature, especially with regard to sky view factor (SVF) upper boundaries. Although the LCZ classification scheme was originally designed to describe local climates with respect to air temperature, our analysis shows that much can be learned from investigating land surface temperature (LST) in these zones. This study serves as a substantial new resource laying a foundation for assessing the SUHI in cities using the LCZ scheme, which could inform climate simulations at local and regional scales.

© 2018 The Authors. Published by Elsevier B.V. on behalf of International Society for Photogrammetry and Remote Sensing, Inc. (ISPRS). This is an open access article under the CC BY-NC-ND license (http://creativecommons.org/licenses/by-nc-nd/4.0/).

1. Introduction

The urban heat island (UHI) effect is defined as the phenomenon that an urban area is significantly warmer than its rural surroundings. UHI magnitude is conventionally quantified through UHI intensity, denoted as $\Delta T_{\text{u-r, max}}$, which is defined as the maximum difference between the urban air temperature and the surrounding rural background (Oke, 1973) using either 2-m air temperature measured in the urban canopy layer or air temperature measured in the urban boundary layer. In this context, two main issues have been found for the use of air temperature data collected from fixed weather stations at screen height. First, "urban" or "rural" has no single, objective meaning because the urban-rural system is complex, and the boundary is always fuzzy (Stewart and Oke, 2012; Unger et al., 2014). Second, air temperature data collected from various sites in the urban area can yield different $\Delta T_{\text{u-r, max}}$ values due to distinctive thermodynamic characteristics of surface materials and local surroundings (Stewart and Oke, 2012; Alexander and Mills, 2014). It is therefore difficult to compare results across cities. To facilitate inter-site comparison and improve the effectiveness of measuring the magnitude of the UHI effect in cities around the world, Stewart and Oke (2012) proposed a classification scheme named Local Climate Zones (LCZs) that comprises 17 classes based on surface cover properties, structure, materials, and human activity. Each LCZ class describes either a built type or a natural land cover type. In addition, the LCZ classification scheme takes geometric, surface cover, thermal, radiative, and metabolic properties into consideration that make each LCZ type unique from the others. The LCZ system can provide a disjoint and complementary partition of the landscape that covers major urban forms and land cover types (Stewart and Oke, 2012; Bechtel et al., 2015a,b).

In recent years, studies have employed the LCZ classification scheme to describe the thermal properties of cities using mobile measurements, weather station data, remotely sensed images, land

* Corresponding author.
E-mail address: ariane.middel@temple.edu (A. Middel).

use and land cover (LULC) data, and urban morphology data acquired from different sources (Bechtel, 2011; Bechtel and Daneke, 2012; Alexander and Mills, 2014; Lelovics et al., 2014; Stewart et al., 2014; Unger et al., 2014; Bechtel et al., 2015a,b, 2016; Leconte et al., 2015; Lehnert et al., 2015; Geletič and Lehnert, 2016; Geletič et al., 2016; Zheng et al., 2017), and reported high effectiveness of this scheme. Yet, few studies to date have been conducted in arid desert cities. Cities such as Phoenix, Arizona and Las Vegas, Nevada, USA, may exhibit lower daytime temperatures than the surrounding desert due to the "oasis effect" that creates a cooling effect (Georgescu et al., 2011; Middel et al., 2014; Fan et al., 2017; Potchter et al., 2008; Hao et al., 2016). It is therefore necessary to evaluate the LCZ classification scheme performance for desert cities in arid environments.

Since the 1960s, with the advent of earth-monitoring satellites and high-resolution digital satellite imagery, remote sensing technology has been widely utilized to assess the surface UHI (SUHI) effect using remotely-sensed land surface temperature (LST), or skin temperature, retrieved from a thermal infrared band image. Satellite images provide continuous data at large spatial coverage, but at a relatively coarse temporal resolution (16 days for ASTER and Landsat data). Although MODIS LST data are collected daily with both daytime and nighttime observations available, the spatial resolution is too coarse. Remotely sensed data also do not fully capture radiant emissions from vertical surfaces such as building walls, because sensors mostly observe energy emitted from horizontal surfaces such as streets, roof tops, and tree tops. Third, observed radiation travels through the thick and dense atmosphere, requiring radiometrical and atmospherical corrections of LST data. Nevertheless, satellite imagery provides fine-scale thermal information that is difficult to obtain through transect measurement campaigns or weather station networks and therefore offer the potential to investigate the SUHI signature of LCZs.

Three popular computer-based approaches to delineate LCZs have been reported in the literature. The first technique is GIS-based (Lelovics et al., 2014; Geletič and Lehnert, 2016) and uses urban structure parameters such as building height, sky view factor (SVF), and building fractions as inputs to be processed in a fuzzy preliminary classification and a post-processing scheme. The output map consists of aggregated LCZ polygons with a minimal size of 500 × 500 m. This method has the aggregation advantage and does not require a selection of training samples. However, the approach requires large amounts of input data that vary in quality and accessibility between cities. The second approach uses satellite remotely sensed data and a classifier, e.g. random forest (Bechtel and Daneke, 2012; Bechtel et al., 2015a). This method is more universal and widely accepted, because input data and software are readily available. It also does not require software expert knowledge and is less computationally demanding. The third method is an integrated approach (Gál et al., 2015) that performs post-classification filtering in addition to the satellite-image based method. It requires a major filter of a specific resolution (100-m), and the preparation of filter input data is time-consuming. Taking all the advantages and disadvantages of different LCZ mapping methods into consideration, this study uses the satellite-image based method for LCZ delineation and mapping, because remotely-sensed imagery has continuous spatial coverage, is available for various dates, and has high spatial resolution.

To promote the concept of LCZ for arid desert cities, this study has three main objectives. The first objective is to classify LCZs for two large desert cities in the Southwestern United States - Phoenix, Arizona and Las Vegas, Nevada using the World Urban Database and Access Portal Tools (WUDAPT) LCZ classification methodology that employs the satellite-image based approach (Bechtel et al., 2015a,b). Second, we calculate LST averages for each LCZ in the two cities to investigate SUHI profiles. Finally, we evaluate LCZ properties for each city based on the attribute ranges proposed by Stewart and Oke (2012).

2. Study area

Phoenix, Arizona and Las Vegas, Nevada (Fig. 1) are large cities in the Southwestern United States, typical of hot, subtropical desert climates (Köppen climate classification: BWh). Phoenix, Arizona is located in the northeast part of the Sonoran Desert and is the fifth largest city in the United States by population. Las Vegas, Nevada (28th largest city in the U.S.) is in a basin on the floor of the Mojave Desert. Both cities are among the hottest of any major city in the United States, characterized by long, hot summers, warm transitional seasons, and short, mild to chilly winters. July is the warmest month with an average high temperature of 41.2 °C in Phoenix and 40.1 °C in Las Vegas (U.S. Climate Data, 2017). Winter months feature mean daily high temperatures above 13 °C and low temperatures rarely below 4 °C.

The average annual precipitation over the past 30 years was 204 mm (8.04 in.) for Phoenix and 106 mm (4.17 in.) for Las Vegas (U.S. Climate Data, 2017), respectively. Phoenix has higher precipitation than Las Vegas due to the North American Monsoon that normally occurs between early July and early September (Adams and Comrie, 1997). The monsoonal moisture influx increases humidity, thunderstorm activity, and can precipitate heavy rainfall and cause extensive flooding. The highest mean daily precipitation in Phoenix occurs in July and August with monthly averages of over 23 mm (Balling and Brazel, 1987; Vivoni et al., 2008). Most of the annual precipitation in Las Vegas falls during the winter months, but even the wettest month (February) averages only four days of measurable rain. Las Vegas is among the sunniest, driest, and least humid locations in North America, with exceptionally low dew points and humidity that sometimes remains below 10%. Winds are generally light, but are normally higher in Las Vegas than Phoenix, both with well-defined diurnal wind regimes (Stewart et al., 2002). On average, winds are 3–5 m/s in Las Vegas, and 1–3 m/s in Phoenix.

Another important characteristic shared by both cities, discussed below, is the similarity in urban morphology and major LULC types that include open soil, grass, trees, paved and impervious surfaces, commercial, industrial, and residential areas (Myint et al., 2015; Wang et al., 2016).

3. Data and methods

3.1. Local climate zone classification

Using the full definition and surface property values of LCZs proposed by Stewart and Oke (2012) as guidance, together with supplemental aerial photographs, this study classified LCZs for the Phoenix and Las Vegas metropolitan areas except built types 1 (compact high-rise), 2 (compact midrise), and 3 (compact low-rise) for both cities and land cover type A (dense trees) for Las Vegas, because preliminary evaluation indicated these LCZ classes are rarely found in the two cities.

Training samples for the LCZ classification were selected using high spatial resolution satellite imagery in Google Earth. The number of training samples was determined proportionally to the area percentage of each LCZ in each city (Table 1). This study follows the World Urban Database and Access Portal Tools (WUDAPT) method proposed by Bechtel et al. (2015a,b) using SAGA GIS to perform the LCZ classification. For the regions of interest in each metropolitan area, cloud free Landsat 8 images were retrieved for all four seasons for 2014–2016 (Table 2) and resampled to 100-meter resolution. Then, the "Local Climate Zone Classification tool" was
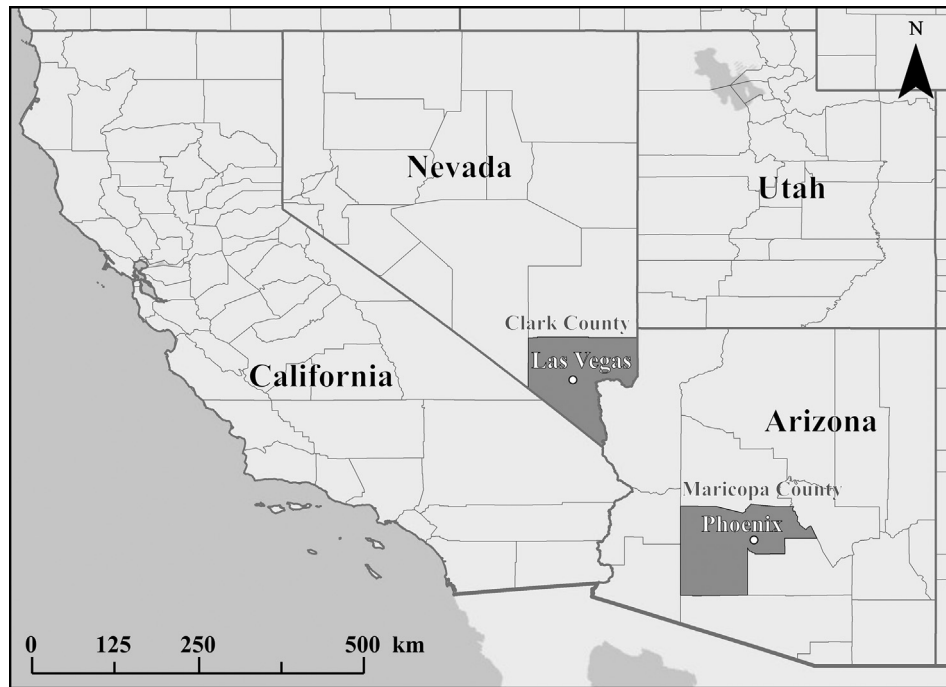
Fig. 1. Map of study area showing Phoenix, Arizona and Las Vegas, Nevada in the Southwest U.S.

Table 1
Number of training samples used for each LCZ and each city.

LCZ	Phoenix	Las Vegas	LCZ	Phoenix	Las Vegas
4: open high-rise	11	29	A: dense trees	29	–
5: open midrise	61	46	B: scattered trees	37	24
6: open low-rise	202	117	C: bush, scrub	40	30
7: lightweight low-rise	49	16	D: low plants	92	64
8: large low-rise	120	73	E: bare rock or paved	23	39
9: sparsely built	45	25	F: bare soil or sand	107	150
10: heavy industry	11	30	G: water	26	9

Table 2
Data description.

Analysis	Data	Resolution	Date Las Vegas	Phoenix
LCZ classification	Landsat	100 m	02/2014–03/2016	04/2014–12/2014
	Google earth	(resampled)		
LULC classification	OrbView-5 (GeoEye-1)	1.65 m	10/12/2011	–
	NAIP	1 m	–	06/07/2010–09/10/2010
SVF	Google street view	Street-level	2015	2015
LST	ASTER (AST_08)	90 m	05/13/2015 (daytime)	05/11/2014 (daytime)
			08/11/2016 (nighttime)	05/31/2015 (nighttime)

executed in SAGA GIS, which uses a random forest classifier to generate LCZs based on the resampled Landsat images and selected training areas.

To perform an accuracy assessment, a total of 1000 validation points were randomly selected for each city based on the classified LCZ map. The number of validation points of each LCZ class was determined proportionally to its area fraction. The classified LCZ maps were compared with Google Earth imagery at each validation point. User's accuracy, producer's accuracy, overall accuracy, and the Kappa coefficient were calculated based on the confusion matrix.

3.2. Evaluation of geometric and surface cover properties for LCZs using LULC and SVF data

Stewart and Oke (2012) suggested value ranges of geometric and surface cover properties for LCZ classes. Using available datasets and products, this study evaluated four surface properties for the LCZ classification of Phoenix and Las Vegas: building surface fraction, impervious surface fraction, pervious surface fraction, and SVF.

The surface area fraction values were derived from LULC maps. The LULC classification for Las Vegas (Fig. 2b) was performed using
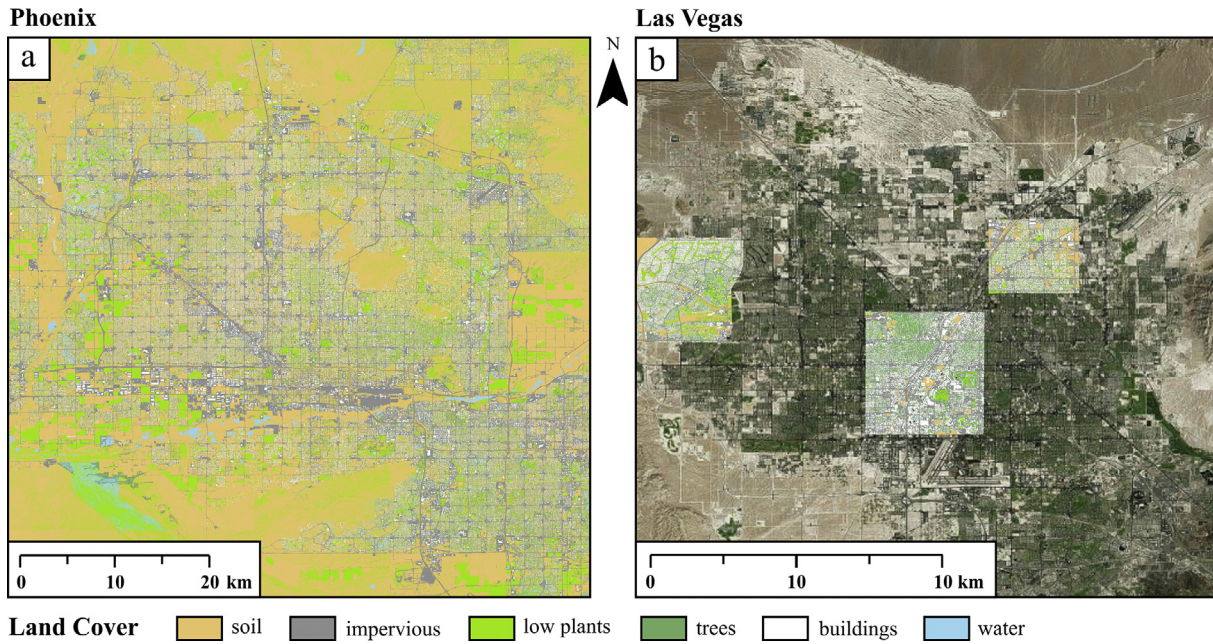
Phoenix

Las Vegas

Land Cover ▢ soil ▢ impervious ▢ low plants ▢ trees ▢ buildings ▢ water

Fig. 2. Classified LULC maps for Phoenix (a) and Las Vegas (b).

an object-oriented image classification technique performed on an OrbView-5 satellite (GeoEye-1) image, acquired on October 12, 2011 with 1.65-meter spatial resolution. Three regional subsets were selected for further analysis, including a typical residential area on the city-desert fringe, the Strip (downtown area), and a mixed residential-industrial zone. Each subset was classified into 6 major LULC types: soil, impervious surface, low plants, trees, buildings, and water. Accuracy was evaluated using stratified-random points with a minimum of 50 points per class. The overall accuracy was 82.8% for the fringe area, 84.8% for the Strip, and 75.0% for the industrial zone.

The Phoenix LULC classification (Fig. 2a) was performed using 2010 National Agriculture Imagery Program (NAIP) imagery with

1-meter spatial resolution that is publicly available through the Central Arizona-Phoenix Long-Term Ecological Research (CAP LTER) website at https://sustainability.asu.edu/caplter/data/view/knb-lter-cap.623.1/. Detailed classification methods and metadata can also be found on this website. The original map has 13 classes with an overall accuracy of 91.9% (CAP LTER, 2015). Some classes were manually grouped together to match the Las Vegas classification scheme.

The street-level SVF was calculated for the Phoenix (Fig. 3a) and Las Vegas (Fig. 3b) metropolitan areas using a method presented by Middel et al. (2017, 2018, in press). 90-degree field-of-view images in each cardinal direction and upwards were retrieved from Google Street View images for any location where images are available.
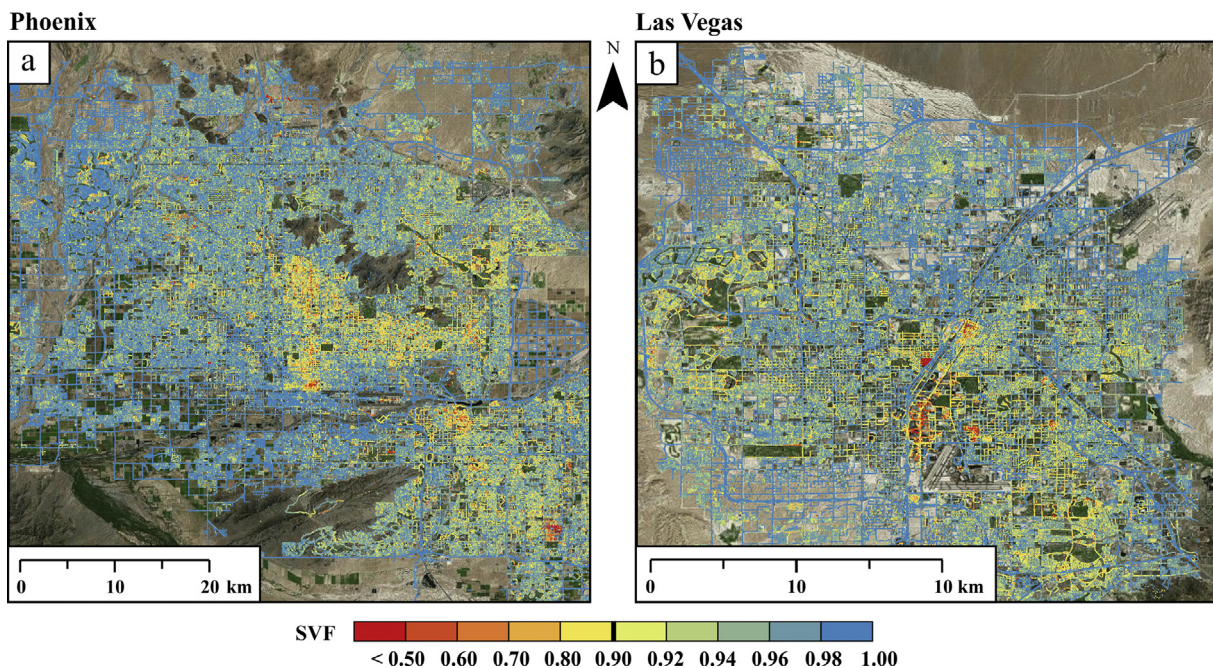
Phoenix

Las Vegas

SVF ▮ < 0.50 0.60 0.70 0.80 0.90 0.92 0.94 0.96 0.98 1.00

Fig. 3. Street-level SVF maps for Phoenix (a) and Las Vegas (b).

The images were projected onto a hemisphere using equiangular projection, and sky pixels were detected using image processing. SVF was then calculated using the modified Steyn method (Middel et al., 2017, 2008, in press). Based on LULC data, three surface cover property maps were generated for both cities by calculating the area percentages of buildings, impervious surface, and pervious surface within every single $100 \times 100\,m$ pixel of the LCZ classification map. These surface cover property maps and the SVF map were then intersected with the LCZ map to evaluate the mean building surface fraction, mean impervious surface fraction, mean pervious surface fraction, and mean SVF for each LCZ in each city, respectively. These mean values were then compared to suggested attribute ranges proposed by Stewart and Oke (2012).

3.3. Evaluation of thermal differentiation for LCZs using land surface temperature data

Air temperature data are the numerical basis of the logical structure of the LCZ system. Stewart and Oke (2012) used mobile air temperature observations from three cities to measure thermal contrasts among LCZ classes. LST was not considered initially, because LCZs are defined based on typical air temperature profiles. Here, we investigate if LCZs also exhibit a typical LST signature. LST data can be derived from remotely sensed thermal infrared (TIR) satellite images. One widely used product is the Advanced Spaceborne Thermal Emission and Reflection Radiometer (ASTER) surface kinetic temperature product (AST_08) (Middel et al., 2012; Myint et al., 2015). AST_08 is processed, calibrated, and distributed by NASA and USGS (NASA LP DAAC 2001) and is corrected using the normalized emissivity method (NEM) (Gillespie et al., 1999). More details on the ASTER LST calculation procedure can be found on the ASTER LST product webpage at https://lpdaac.usgs.gov/dataset_discovery/aster/aster_products_table/ast_08_v003. Based on availability and image quality, scenes acquired on May 31, 2015 (Fig. 4a) and May 11, 2014 (Fig. 4c) were used for Phoenix for the daytime (10:30 a.m.) and nighttime (10:30 p.m.) LST analysis, respectively. For Las Vegas, May 13, 2015 (Fig. 4b) and August 11, 2016 (Fig. 4d) images were used for the daytime and nighttime LST analysis, respectively. The ASTER scene acquisition dates match the Landsat 8 image acquisition dates that were used for the LCZ classification. Pixel values were converted from kinetic temperature in Kelvin to degrees Celsius. The minimum LST, maximum LST, mean LST, and standard deviations were then calculated for each LCZ class in each city.

4. Results

4.1. LCZ classification result

Fig. 5 shows LCZ maps for Phoenix (Fig. 5a) and Las Vegas (Fig. 5b), and Table 3 shows error matrices for the classification accuracy assessment. The overall accuracy of the LCZ classification is 81.5% and 81.9% for Phoenix and Las Vegas, respectively. The Kappa coefficient value is 0.792 for Phoenix and 0.788 for Las Vegas, representing an overall satisfactory classification result.

Fourteen LCZs were classified for each city. Fig. 6 shows examples of all LCZs using high resolution imagery from Google Earth to provide a visual representation of each LCZ in a desert city. The area proportion of each LCZ in each city is shown in Table 4. The largest and the second largest LCZs in both cities are bare soil/sand and open low-rise, respectively, which together cover around 80% of the total metropolitan area. The urbanization process of a desert city is more inclined to horizontal expansion rather than vertical development, because more land is available for development than in other major U.S. cities. Therefore, open low-rise and large

low-rise buildings are the predominant building types in Phoenix and Las Vegas.

LCZ B (scattered trees) has the smallest coverage in both cities, as trees are naturally scarce in a desert environment. The predominant vegetation types are bush, shrub, and grass. The area of the low plant LCZ in Phoenix is larger than any other vegetated area, because Phoenix has active agriculture in rural areas all year round, while agriculture is rarely found in Las Vegas.

The pairwise correlation coefficient r is 0.9913 for the LCZ area proportions between Phoenix and Las Vegas. The correlation is highly statistically significant (p-value < 0.01), meaning the LCZ composition and urban structure of the two cities are very similar.

4.2. Geometric and surface cover properties of LCZ classes in Phoenix and Las Vegas

The mean values of geometric and surface cover properties per LCZ for both cities are listed in Table 5. The highlighted values are either more than 20% lower than the lower end of the value range or more than 20% higher than the higher end of the value range proposed by Stewart and Oke (2012). All the other values are considered acceptable in this study. For the building fraction, most of the LCZs are within or close to the value ranges except lightweight low-rise, sparsely built, and heavy industry LCZs. These three LCZs have significantly lower building fractions than the standard, because these LCZs are mostly found on the city outskirts or in far rural areas where building density is much lower than in the urban area. Especially in the sparsely built LCZ (see LCZ 9 in Fig. 6), buildings are spaced out and are surrounded by desert open soil and shrubs. This explains why the pervious fraction is significantly higher than the range for this LCZ. All natural land cover LCZs meet the standard and have less than 10% building surface fraction in both cities.

The lightweight low-rise LCZ exhibits significantly higher impervious fractions than the standard. This is because most lightweight low-rise buildings in the two cities (see LCZ 7 in Fig. 6), such as mobile park homes and temporary homes on construction sites, have surroundings that are well-paved using impervious materials such as asphalt and bricks. The heavy industry LCZ in Las Vegas has a significantly lower impervious fraction than the standard. Most industrial areas in Las Vegas are non-paved, and soil is exposed (see LCZ 10 in Fig. 6), especially in rock quarries and mining fields. This also explains why the pervious fraction for the heavy industry is significantly higher than the proposed value range. All the other built type LCZs and land cover type LCZs are within the acceptable range of the standard.

The sparsely built and heavy industry LCZs are the only two zones that have a significantly higher average pervious fraction than the value range for reasons explained above. All the other LCZs are within the acceptable range of the standard.

Regarding the SVF, open high-rise, open midrise, lightweight low-rise, dense trees, and scattered trees all have much higher values than the proposed range. Unlike other large cities, the average SVF of open high-rise LCZs in Phoenix and Las Vegas (see LCZ 4 in Fig. 6) is larger than 0.8. This is due to extremely low height-to-width ratios of street canyons in desert cities; roads can have up to 7 lanes. At the same time, high-rise buildings are much shorter than the major towers and skyscrapers in other large U.S. cities. For example, the tallest building in Phoenix is the 40-story Chase Tower, which only rises 147 m above the ground. Las Vegas has more than 160 high-rises, but they spread out along the Las Vegas Strip instead of being densely situated in a few blocks. In addition, trees in a desert environment have much smaller canopy closure. Both horizontal and vertical spaces are therefore wide open leading to larger SVFs in Phoenix and Las Vegas than in other major
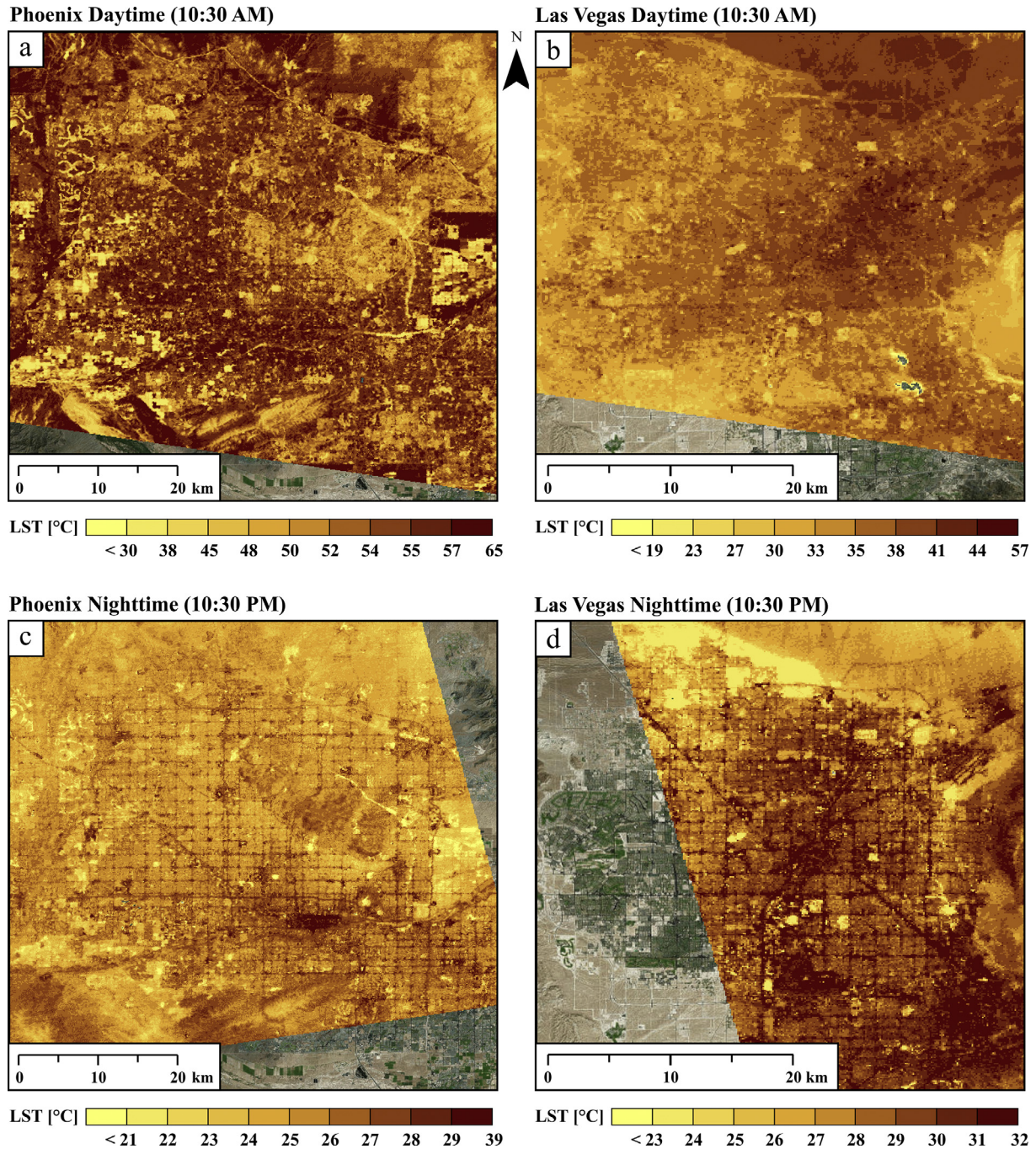
Phoenix Daytime (10:30 AM)

Las Vegas Daytime (10:30 AM)

Phoenix Nighttime (10:30 PM)

Las Vegas Nighttime (10:30 PM)

Fig. 4. LST images from ASTER satellite for Phoenix (a and c) and Las Vegas (b and d).

U.S. cities. Middel et al. (2018, in press) found that both cities rank highest in SVF footprints calculated from Google Street View images for 15 cities around the globe.

4.3. Thermal differentiation of LCZ classes in Phoenix and Las Vegas

Table 6 shows summary statistics of daytime and nighttime LST for each LCZ and city. For the Phoenix metropolitan area, the bare rock or paved LCZ has the highest LST during daytime and nighttime among all LCZs. The large low-rise LCZ has the highest LST at daytime, and the open high-rise LCZ has the highest LST at nighttime in all built types. Water and low plants have the lowest LST at daytime and nighttime, respectively. Open high-rise has the lowest

LST among all built types during daytime, while sparsely built has the lowest LST at night.

Las Vegas has a similar LST pattern. Large low-rise is among the hottest zones for both daytime and nighttime in all LCZs, and the open high-rise LCZ has the highest LST at nighttime among all built types. Water has the lowest LST during daytime, while the bush and scrub LCZ has the lowest LST at nighttime.

Fig. 7 shows the departure from the mean LST for all LCZ classes. Water, low plants, scattered trees, and dense trees have consistently cooler mean LST than all other LCZ classes during daytime and nighttime in both cities, with water being the coolest. Bare rock or paved and large low-rise LCZs show a larger LST departure from the mean for both daytime and nighttime in both cities. Open
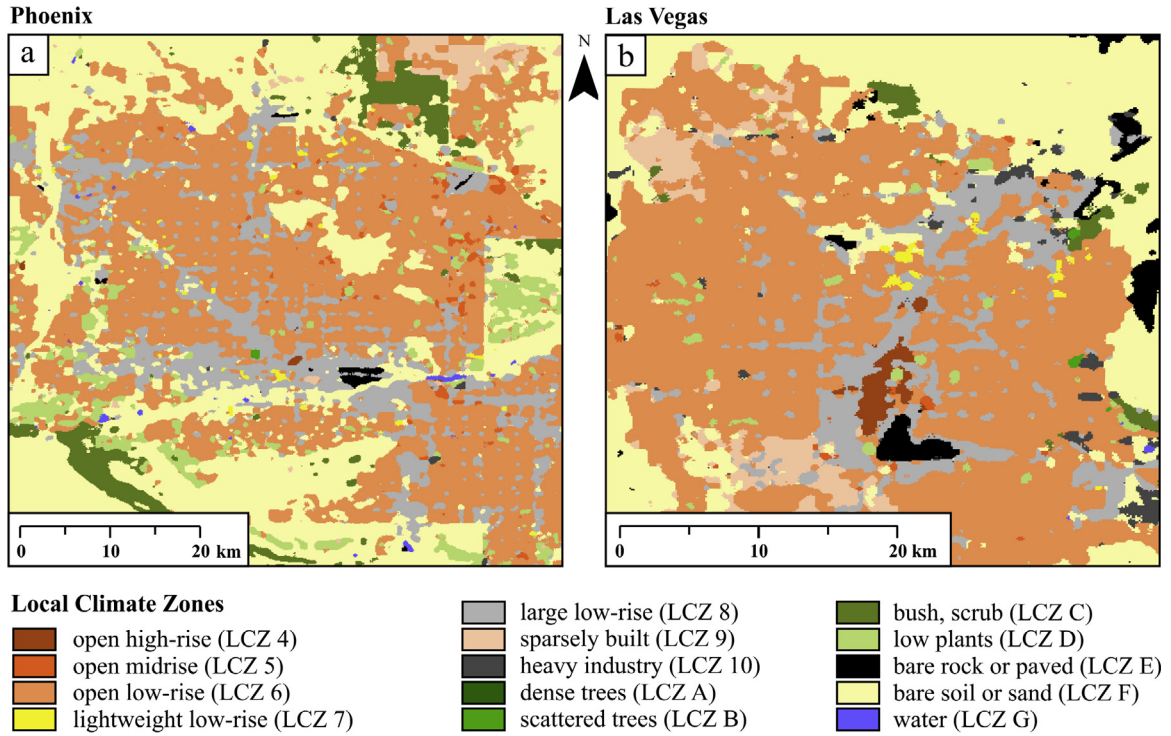
Phoenix

Las Vegas

Local Climate Zones

- open high-rise (LCZ 4)
- open midrise (LCZ 5)
- open low-rise (LCZ 6)
- lightweight low-rise (LCZ 7)
- large low-rise (LCZ 8)
- sparsely built (LCZ 9)
- heavy industry (LCZ 10)
- dense trees (LCZ A)
- scattered trees (LCZ B)
- bush, scrub (LCZ C)
- low plants (LCZ D)
- bare rock or paved (LCZ E)
- bare soil or sand (LCZ F)
- water (LCZ G)

Fig. 5. LCZ classification for Phoenix (a) and Las Vegas (b).

Table 3
Confusion matrix of the LCZ classification for Phoenix and Las Vegas; Overall accuracy of the LCZ classification is 81.5% for Phoenix and 81.9% for Las Vegas; Kappa coefficient is 0.792 for Phoenix and 0.788 for Las Vegas.

Phoenix

	Ground Truth																
	LCZ 4	LCZ 5	LCZ 6	LCZ 7	LCZ 8	LCZ 9	LCZ 10	LCZ A	LCZ B	LCZ C	LCZ D	LCZ E	LCZ F	LCZ G	Row total	User's accuracy
LCZ 4	25	0	0	0	0	0	0	0	0	0	0	0	0	0	25	100.0%
LCZ 5	0	30	1	0	10	0	0	0	0	0	0	0	0	0	41	73.2%
LCZ 6	0	19	88	18	20	2	2	0	0	0	1	0	1	1	152	57.9%
LCZ 7	0	0	0	30	0	0	0	0	0	0	0	0	0	0	30	100.0%
LCZ 8	0	0	3	0	62	0	1	0	0	0	0	0	0	0	66	93.9%
LCZ 9	0	0	0	0	0	49	0	0	0	1	0	0	3	0	53	92.5%
LCZ 10	0	0	0	0	1	0	26	0	0	0	0	0	0	0	27	96.3%
LCZ A	0	0	0	0	0	0	0	28	0	0	0	0	0	0	28	100.0%
LCZ B	0	0	0	0	0	0	0	0	17	0	0	0	0	0	17	100.0%
LCZ C	0	0	3	0	2	25	0	1	3	93	1	1	1	0	130	71.5%
LCZ D	0	1	3	0	1	0	1	1	9	3	97	0	0	0	116	83.6%
LCZ E	0	0	0	0	0	0	0	0	0	0	0	29	0	0	29	100.0%
LCZ F	1	0	2	2	4	24	0	0	1	3	1	0	195	3	236	82.6%
LCZ G	4	0	0	0	0	0	0	0	0	0	0	0	0	46	50	92.0%
Column total	30	50	100	50	100	100	30	30	30	100	100	30	200	50	1000	
Producer's accuracy	83.3%	60.0%	88.0%	60.0%	62.0%	49.0%	86.7%	93.3%	56.7%	93.0%	97.0%	96.7%	97.5%	92.0%		

(Classified as — row labels)

Las Vegas

	Ground Truth															
	LCZ 4	LCZ 5	LCZ 6	LCZ 7	LCZ 8	LCZ 9	LCZ 10	LCZ B	LCZ C	LCZ D	LCZ E	LCZ F	LCZ G	Row total	User's accuracy
LCZ 4	24	0	0	0	0	0	0	0	0	0	0	0	0	24	100.0%
LCZ 5	4	19	2	0	5	0	0	0	0	0	0	0	0	30	63.3%
LCZ 6	0	2	189	11	9	16	3	0	0	0	3	3	0	236	80.1%
LCZ 7	0	0	0	19	2	0	1	0	0	0	0	0	0	22	86.4%
LCZ 8	2	8	3	0	107	4	2	0	0	1	0	0	0	127	84.3%
LCZ 9	0	0	0	0	0	97	0	0	0	0	0	0	0	97	100.0%
LCZ 10	0	0	0	0	0	1	27	0	0	0	0	0	0	28	96.4%
LCZ B	0	0	0	0	0	0	0	18	0	0	0	0	0	18	100.0%
LCZ C	0	0	0	0	0	0	0	0	21	0	0	0	0	21	100.0%
LCZ D	0	0	1	0	0	2	0	2	0	28	0	0	0	33	84.8%
LCZ E	0	0	1	0	9	1	3	0	1	1	47	1	0	64	73.4%
LCZ F	0	1	3	0	18	28	14	0	8	0	0	196	3	271	72.3%
LCZ G	0	0	1	0	0	1	0	0	0	0	0	0	27	29	93.1%
Column total	30	30	200	30	150	150	50	20	30	30	50	200	30	1000	
Producer's accuracy	80.0%	63.3%	94.5%	63.3%	71.3%	64.7%	54.0%	90.0%	70.0%	93.3%	94.0%	98.0%	90.0%		

LCZ 4 open high-rise

LCZ 7 lightweight low-rise

LCZ 10 heavy industry

LCZ B scattered trees

LCZ E bare rock or paved

LCZ 5 open midrise

LCZ 8 large low-rise

built types

LCZ C bush, scrub

LCZ F bare soil or sand

land cover types

LCZ 6 open low-rise

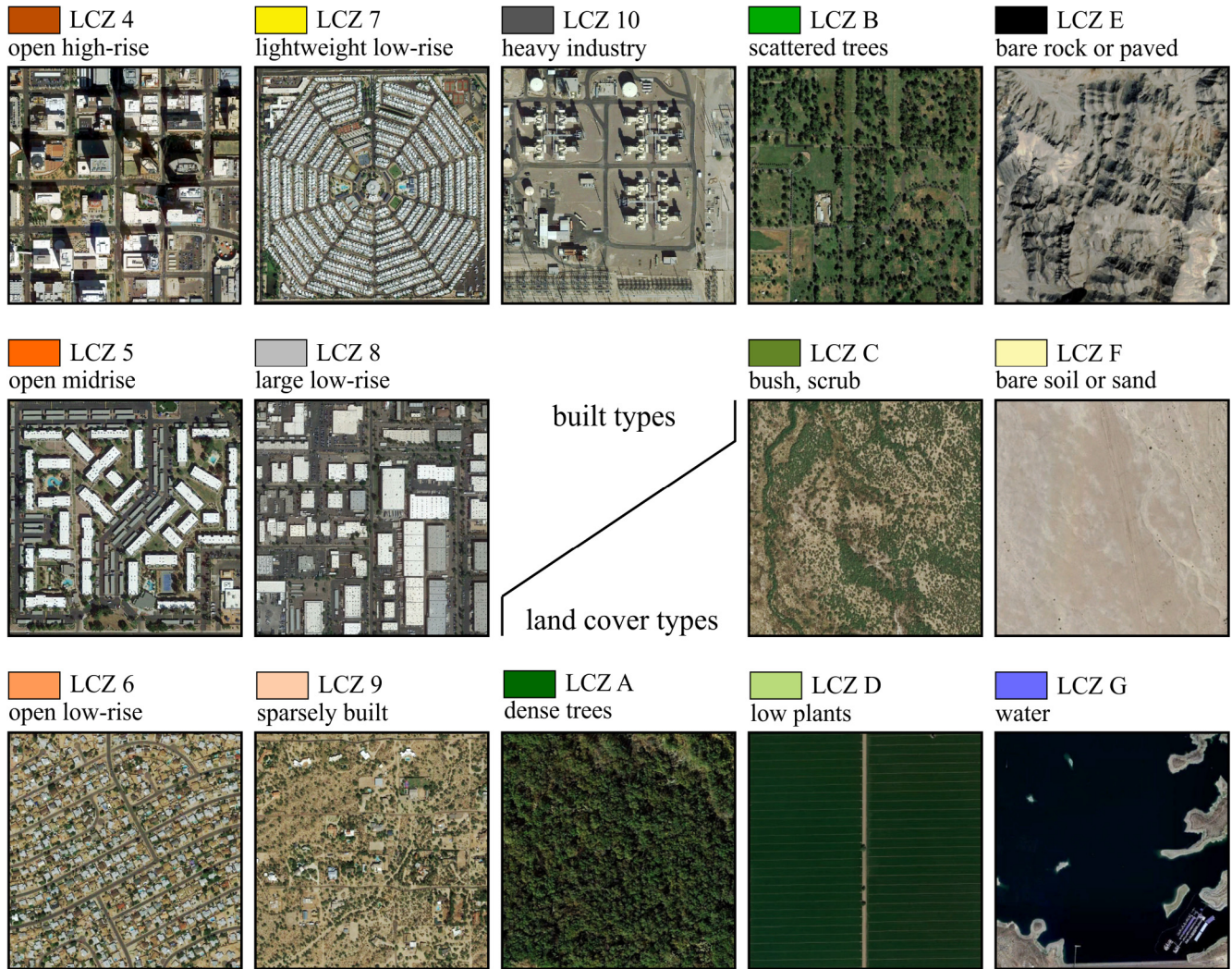LCZ 9 sparsely built

LCZ A dense trees

LCZ D low plants

LCZ G water

Fig. 6. Examples of LCZs in Phoenix and Las Vegas from Google Earth imagery.

Table 4
Area proportion of each LCZ in Phoenix and Las Vegas (unit: %).

LCZ	Phoenix	Las Vegas	LCZ	Phoenix	Las Vegas
4:open high-rise	0.03	0.55	A:dense trees	0.08	–
5:open midrise	0.52	0.14	B:scattered trees	0.02	0.05
6:open low-rise	33.07	34.15	C:bush, scrub	3.72	0.77
7:lightweight low-rise	0.48	0.23	D:low plants	3.98	0.67
8:large low-rise	8.19	6.05	E:bare rock or paved	0.16	3.69
9:sparsely built	2.83	5.48	F:bare soil or sand	46.70	46.97
10:heavy industry	0.07	1.18	G:water	0.14	0.08

midrise and open high-rise LCZs are the coolest zones with respect to LST among all built types.

5. Discussion

5.1. Evaluation of the LCZ classification for desert cities

It has been commonly accepted that a target accuracy of 85% is necessary for thematic mapping via classification analysis using remotely sensed images (Anderson, 1976; McCormick, 1999; Scepan, 1999; Foody, 2002, 2008; Wulder et al., 2006). Although the overall accuracy of our classified LCZ maps is lower than 85%

for both cities, it can be argued that this study was not designed for a thematic mapping of major LULC classes, but for the newly developed concept of LCZs. Other studies have classified cities into LCZs using various datasets including multitemporal and multispectral satellite images, synthetic aperture radar (SAR) data, weather station data, and mobile measurements, employing different methods and classifiers to retrieve LCZs for a city at different scales (Bechtel, 2011; Bechtel and Daneke, 2012; Alexander and Mills, 2014; Lehnert et al., 2015; Leconte et al., 2015; Bechtel et al., 2016). Bechtel et al. (2016) used a combination of multispectral, TIR, and SAR data to perform a LCZ classification and reported overall accuracies between 50.9% and 98.3%. Bechtel et al. (2015a, b) used the same classification method as this study to perform a

Table 5
Geometric and surface cover properties of LCZ classes in Phoenix and Las Vegas compared to Stewart and Oke (2012)'s suggested LCZ parameter ranges.

LCZ	Phoenix	Las Vegas	Stewart&Oke	Phoenix	Las Vegas	Stewart&Oke	Phoenix	Las Vegas	Stewart&Oke	Phoenix	Las Vegas	Stewart&Oke
	Building surface fraction			Impervious surface fraction			Pervious surface fraction			Sky view factor		
LCZ 4 (open high-rise)	20.80%	33.30%	20% - 40%	39.26%	35.37%	30% - 40%	39.94%	31.33%	30% - 40%	0.80	0.82	0.5 - 0.7
LCZ 5 (open midrise)	24.65%	32.02%	20% - 40%	34.20%	35.39%	30% - 50%	41.15%	32.59%	20% - 40%	0.91	0.92	0.5 - 0.8
LCZ 6 (open low-rise)	17.34%	32.81%	20% - 40%	21.08%	27.05%	20% - 50%	61.58%	40.14%	30% - 60%	0.97	0.94	0.6 - 0.9
LCZ 7 (lightweight low-rise)	26.97%	35.73%	60% - 90%	37.54%	31.96%	<20%	35.49%	32.31%	<30%	0.96	0.95	0.2 - 0.5
LCZ 8 (large low-rise)	28.71%	31.07%	30% - 50%	50.23%	48.28%	40% - 50%	21.06%	20.65%	<20%	0.94	0.94	>0.7
LCZ 9 (sparsely built)	4.14%	0.33%	10% - 20%	3.93%	0.20%	<20%	91.93%	99.47%	60% - 80%	0.97	0.97	>0.8
LCZ 10 (heavy industry)	6.07%	9.78%	20% - 30%	20.00%	12.04%	20% -40%	73.93%	78.18%	40% - 50%	0.93	0.96	0.6 - 0.9
LCZ A (dense trees)	0.50%	-	<10%	4.44%	-	<10%	95.06%	-	>90%	0.99	-	<0.4
LCZ B (scattered trees)	1.92%	-	<10%	11.22%	-	<10%	86.86%	-	>90%	0.96	0.98	0.5 - 0.8
LCZ C (bush, scrub)	0.17%	-	<10%	0.56%	-	<10%	99.27%	-	>90%	0.98	0.95	0.7 - 0.9
LCZ D (low plants)	0.73%	6.32%	<10%	2.57%	4.46%	<10%	96.70%	89.22%	>90%	0.96	0.91	>0.9
LCZ E (bare rock or paved)	2.26%	0.20%	<10%	88.18%	98.90%	>90%	9.56%	0.90%	<10%	0.96	0.92	>0.9
LCZ F (bare soil or sand)	0.78%	2.60%	<10%	2.64%	3.03%	<10%	96.58%	94.37%	>90%	0.97	0.95	>0.9
LCZ G (water)	0.97%	-	<10%	5.69%	-	<10%	93.34%	-	>90%	-	-	>0.9

Table 6
Summary statistics of LST per LCZ in Phoenix and Las Vegas.

LCZ	Phoenix daytime				Phoenix nighttime				Las Vegas daytime				Las Vegas nighttime			
	Min.	Max.	Mean	Std.	Min.	Max.	Mean	Std.	Min.	Max.	Mean	Std.	Min.	Max.	Mean	Std.
LCZ 4 (open high-rise)	33.2	59.1	49.7	6.2	22.7	29.5	26.8	1.7	19.0	46.9	35.1	3.3	13.3	36.7	31.3	2.3
LCZ 5 (open midrise)	36.8	61.0	51.6	2.7	20.2	29.5	25.4	1.3	23.2	41.0	35.2	3.0	27.1	34.8	31.1	1.3
LCZ 6 (open low-rise)	31.7	63.6	53.0	3.0	17.5	32.1	25.1	1.2	19.0	47.6	36.1	3.2	10.5	38.6	30.3	1.9
LCZ 7 (lightweight low-rise)	42.6	62.1	53.1	2.9	19.4	31.5	24.4	1.5	29.2	44.7	40.4	1.8	24.2	34.3	30.2	1.5
LCZ 8 (large low-rise)	32.3	75.6	55.1	2.7	18.1	42.7	26.4	1.5	19.0	57.2	38.5	3.2	12.9	38.8	31.2	1.9
LCZ 9 (sparsely built)	34.1	60.6	53.2	2.6	17.9	29.5	23.9	1.1	24.3	43.3	34.9	2.8	7.3	34.7	29.7	2.3
LCZ 10 (heavy industry)	40.6	60.2	54.0	3.5	22.1	29.7	26.1	1.4	22.0	48.9	37.0	3.3	7.3	38.0	30.8	2.2
LCZ A (dense trees)	40.8	55.1	47.8	3.6	23.2	25.2	24.2	0.7	19.0	47.6	33.2	3.8	–	–	–	–
LCZ B (scattered trees)	38.1	59.1	47.2	4.5	21.6	27.2	24.7	1.1	29.3	39.6	33.0	1.8	19.3	31.8	24.5	3.3
LCZ C (bush, scrub)	32.7	64.1	54.1	4.7	20.0	28.5	24.6	0.9	23.0	46.8	37.6	3.2	20.4	33.2	27.9	2.9
LCZ D (low plants)	28.1	65.3	46.2	6.5	16.5	29.5	23.0	1.5	20.8	45.2	30.4	3.5	18.0	34.9	26.9	3.0
LCZ E (bare rock or paved)	37.1	62.8	56.6	2.8	21.9	31.4	28.7	1.6	22.3	44.2	34.9	3.7	19.1	38.0	30.4	1.9
LCZ F (bare soil or sand)	26.0	66.2	54.9	3.5	15.5	34.7	24.8	1.2	19.2	47.1	37.5	3.3	10.4	35.9	29.2	2.0
LCZ G (water)	25.2	61.7	31.0	7.2	19.1	28.5	24.2	2.3	17.0	38.3	23.6	5.6	27.1	35.0	30.5	1.5

Departure from Land Surface Temperature Mean

■ Las Vegas nighttime (August 11, 2016)   ■ Las Vegas daytime (May 13,2015)   ■ Phoenix nighttime (May 11, 2014)   ■ Phoenix daytime (May 31, 2015)
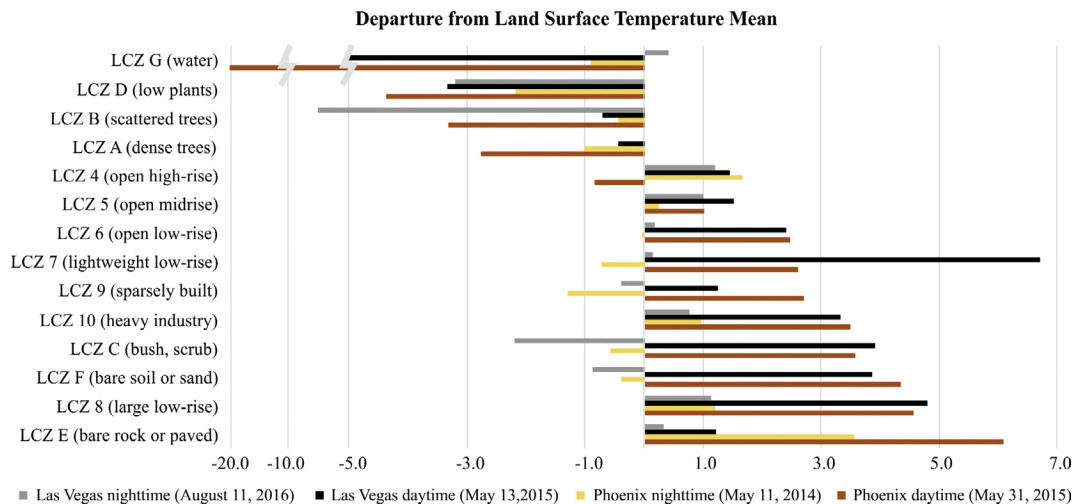
Fig. 7. Departure from the mean LST (unit: °C).

LCZ classification for Huston, Texas, USA and reached an accuracy of 96%, but their assessment was based on training data only. Our classification separated validation data from training data and reached an average overall accuracy of 81.7%, which is therefore considered acceptable. It has to be noted that the classification accuracy for natural classes is generally higher than the accuracy for built classes.

Selecting an appropriate method and representative training and validation areas is crucial for LCZ classifications and subsequent accuracy assessments. The selection of training and

validation polygons is highly dependent on local expert knowledge. People have varying cognitive interpretations of the urban landscape, which can significantly influence the classification result and accuracy. Bechtel et al. (2017) showed this in a LCZ human influence experiment (HUMINEX). Here, we further found that selecting training and validation areas for desert environments is particularly challenging. For example, areas with relatively low coverage of bush and scrub (LCZ C) can be mistakenly recognized as bare soil or sand (LCZ F). Open low-rise (LCZ 6) in a xeric or native desert style neighborhood (see examples in Middel et al., 2014; Song and Wang, 2015) can be mistakenly identified as lightweight low-rise (LCZ 7). An adequate number of samples must be selected to minimize the error. Up to date, the WUDAPT method has been applied to over 50 cities around the world (Bechtel et al., 2015b; Danylo et al., 2016), but the results of only few cities have recently been quantitatively validated to show high mapping accuracies (Danylo et al., 2016; Bechtel et al., 2015a). It is therefore necessary to perform further testing and validation of the WUDAPT method to produce technically and scientifically sound results and to ensure the quality of LCZ products (Verdonck et al., 2017).

Table 3 illustrates considerable confusion between LCZ 6 (open low-rise) and LCZ 7 (lightweight low-rise), and between LCZ 9 (sparsely built) and LCZ F (bare soil or sand) for both cities. Open low-rise residential areas, especially in xeric or native desert style neighborhoods, and lightweight low-rise LCZs in both cities are characterized by single-story buildings surrounded by open soil, grass, shrubs, and a few scattered trees. Although construction materials and building styles are quite different, the landscape design is very similar, which cannot be easily discriminated using resampled Landsat images at 100-m resolution. The sparsely built LCZ in a natural desert environment meets the LCZ definition and criteria (Stewart and Oke, 2012), but it has no significant spectral difference from open soil and sand, because the area proportion of buildings to desert is too small. It is also found that in Phoenix, LCZ 6 (open low-rise) has the lowest user's accuracy. LCZ 6 was most often confused with LCZ 8 (large low-rise). Unger et al. (2014) also reported that properties of open low-rise and large low-rise LCZs were found to be similar for Szeged, Hungary, which is in a marine west coast climate zone (Köppen climate classification: Cfb). Bechtel et al. (2015a,b) also found misclassifications between these two LCZ classes in Houston, Texas, USA. Therefore, the confusions between LCZs is a common issue found in many cities that is not only caused by the environmental background.

5.2. LCZ properties

The geometric and surface cover properties of classified LCZs in Phoenix and Las Vegas generally correspond well to those proposed by Stewart and Oke (2012). Nevertheless, some significant differences were found due to the unique desert urban morphology. Our findings suggest that the value ranges for selected LCZs should be treated as guidelines and could potentially be adjusted to better reflect the desert morphology. Leconte et al. (2015) also found discrepancies between observed and suggested geometric and surface cover properties, reporting that variations may be caused by different geometric layouts and the amount of greenery of specific local features. Geletič and Lehnert (2016) studied LCZs for three mid-sized Central European cities and suggested that, with respect to the LCZ classification method and procedure, it is necessary to take specific regional features and the morphological character of built-up areas into account. Adjusting some surface fraction intervals and property values seems reasonable when working with different cities of different regional climate (Geletič and Lehnert, 2016).

Fig. 8 shows that the lightweight low-rise (LCZ 7) built type exhibits geometric and surface cover properties that fit well into the range of open low-rise (LCZ 6). In addition, sparsely built (LCZ 9) is very similar to bare soil or sand (LCZ F). Therefore, additional information beyond Landsat data (e.g., Sentinels or ASTER) and improved methods, such as a contextual classifier (Verdonck et al., 2017) are needed to distinguish those zones. Our study results suggest that multispectral optical and multitemporal remotely sensed data may not be sufficient for cities in arid desert climate regions. Additional datasets, such as TIR and SAR data, are necessary to differentiate classes between sparsely built and open low-rise, and between open low-rise and large low-rise (Bechtel et al., 2016). In addition, SAR data can assist to distinguish built type LCZ classes of different heights and surface roughness.

The SVF is an important indicator of urban morphology for the LCZ classification. We found that LCZ classes 4, 5, 6, 7, A, and B exhibit SVF values that are significantly higher than the proposed value ranges. We acknowledge that the employed SVF approach is biased towards street canyons and disregards sky obstructions in parks, backyards, and open spaces. Although Google has started to acquire panoramic imagery on hiking trails, university campuses, and pedestrian areas attractive to tourists, current Street View images are not representative of the full spatial extent of a city, and coverage of rural areas and forests is even sparser. Therefore, the SVF evaluation method based on Street View images should be limited to urban, built-up LCZs. We recommend that the upper boundaries for SVF ranges should be further tested for all built-type LCZ classes for sprawled desert cities, possibly using other data products such as LIDAR data in support.

5.3. Thermal differentiation of LCZs and implications for the surface urban heat island effect

Stewart et al. (2014) encouraged LCZ evaluation studies for urban environments under various climatic conditions using observations and model simulations. One of the advantages using LST data is the ability to adequately represent continuous surface temperature for both daytime and nighttime for large geographic areas. The WUDAPT method includes the Landsat thermal band image to perform LCZ classifications, which could be a potential source of a methodological bias in the LST analysis. To minimize this bias, we used LST data derived from a different satellite sensor (ASTER) that has other data collection dates and times, a different spatial resolution, and different spectral wavelengths. One issue that remains though is the LST variation with sensor view angle, resulting in an effective anisotropy of surface thermal emission (Vinnikov et al., 2012; Krayenhoff and Voogt, 2016; Dyce and Voogt, 2018). Krayenhoff and Voogt (2016) modeled anisotropy for various LCZs using TUF3D-SUM and found a maximum anisotropy magnitude of 8 K for compact high-rise neighborhoods and around 3 K for open lowrise neighborhoods at 30° Latitude during daytime. Anisotropy is important to consider in assessing absolute surface temperatures derived from remotely sensed products but is of lesser concern in this study. First, anisotropy does not significantly impact LST results during nighttime; second, most Phoenix and Las Vegas LCZs fall into the open low-rise category, which has a reduced anisotropy.

Geletič et al. (2016) examined daytime LST differences for LCZs in Prague and Brno, Czech Republic. They found that heavy industry (LCZ 10), compact low-rise buildings (LCZ 3) and compact mid-rise buildings (LCZ 2) had the highest LST in both cities, while water bodies (LCZ G) and dense trees (LCZ A) had the lowest. The LCZ classification results in this study do not include compact zones, but the highest average LST was found in the bare rock or paved LCZ (LCZ E), while the lowest LST was observed in the low
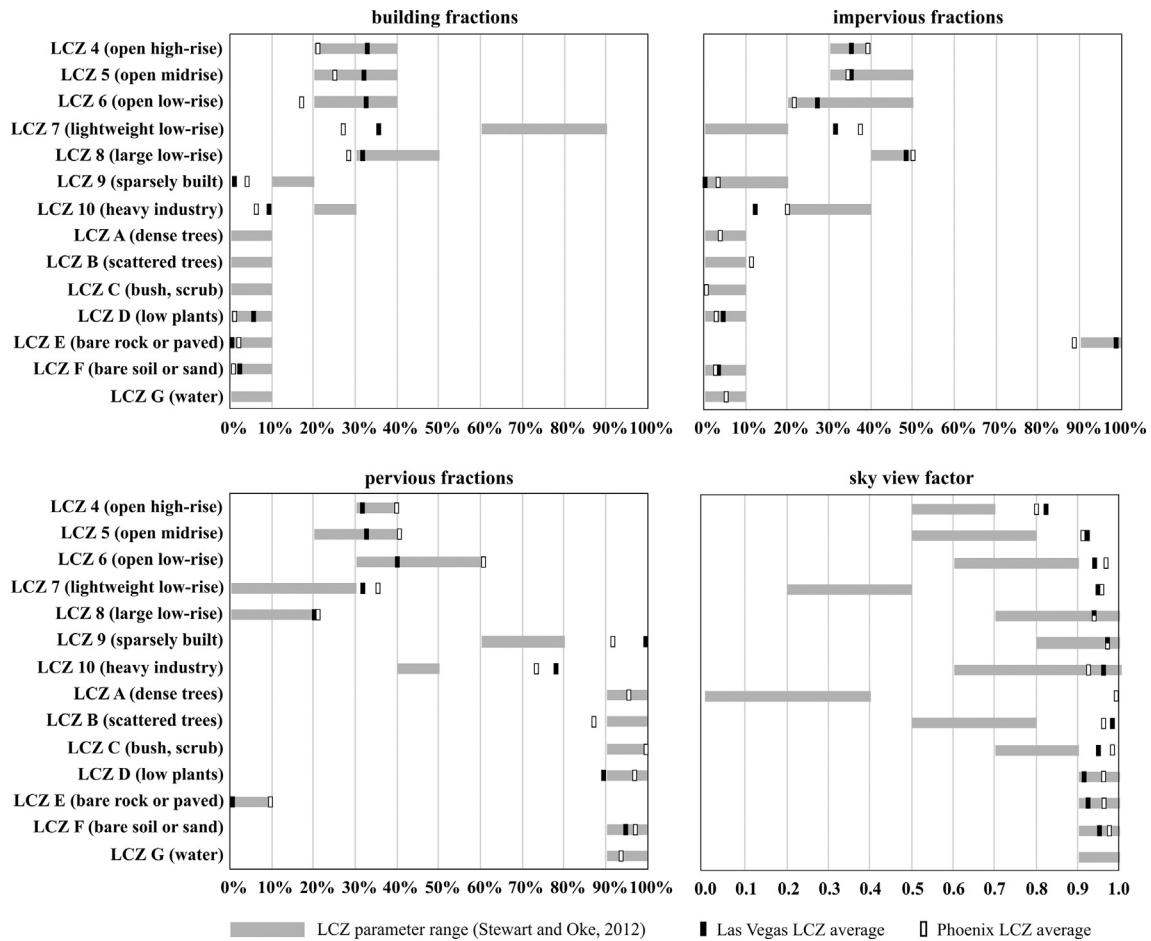
Fig. 8. Geometric and surface cover properties of LCZ classes in Phoenix and Las Vegas compared to Stewart and Oke (2012)'s suggested LCZ parameter ranges.

plants zone (LCZ D). These differences are due to the unique desert urban environment and morphology of our study areas. Our study conducts separate analyses for daytime and nighttime LST rather than daytime only; this facilitates further understanding of how LST and the SUHI vary temporally.

Alexander and Mills (2014) analyzed thermal properties for LCZs in Dublin, Ireland, and Leconte et al. (2015) evaluated LCZs for Nancy, France using air temperature. Both studies found that low plants (LCZ D) were consistently cooler during daytime, while LCZs with high impervious and building fractions were the warmest. Our analysis shows the same result for both Phoenix and Las Vegas LST, although the U.S. Southwest climate is quite different from Ireland and France. Vegetation lowers air temperature by evapotranspiration and shading, but it also exhibits lower LST than other urban fractions. Therefore, increasing green space is known to be an effective UHI and SUHI mitigation strategy (Rosenfeld et al., 1995; Ca et al., 1998; Ashie et al., 1999; Tong et al., 2005; Yu and Hien, 2006; Yuan and Bauer, 2007; Kong et al., 2016). Both bare rock and paved zones (LCZ E) are mainly impervious with a low infiltration rate. Recent studies found that dark impervious surfaces are the primary cause of SUHI effects in Phoenix (Myint et al., 2013; Wang et al., 2016). This corresponds to our findings that LCZs with higher impervious fractions exhibit higher LST than other zones.

However, our LST results do not compare well with air temperature results for some of the built zones. Lelovics et al. (2014) found high-rise and mid-rise LCZs to be warmer than low-rise zones. In contrast, our LST ranking from the highest to lowest LST is low-rise, midrise, and high-rise for both cities during the

day and a reversed order at night. High-rise buildings are mainly found in downtown areas for both Phoenix and Las Vegas. Downtown street canyons potentially create a daytime cooling effect through shading (Pearlmutter et al., 2009; Middel et al., 2014). At night, absorbed shortwave radiation that is stored as heat in buildings and impervious surfaces during the day is slowly released after sunset in the form of longwave radiation that heats up the lower atmosphere (Oke, 1982; Mills, 1999; Bouyer et al., 2009), but the stored heat also manifests itself in higher LST values. Similar to the UHI, the SUHI effect is very pronounced during the evening in a desert city (Wang et al., 2016). The low-rise LCZs in a desert environment do not provide much shade during the daytime, which leads to higher LST, but the stored heat can be quickly released after sunset due to high SVFs, so the surface cools down faster than midrise and high-rise LCZs.

6. Conclusions

This study classified and evaluated LCZs for Phoenix and Las Vegas using the satellite image-based LCZ classification method developed by Bechtel et al. (2015a,b). Seven built-type LCZs and seven lateral land cover type LCZs were identified, and the LCZs' geometric, surface cover, and thermal properties were evaluated using SVF, LULC, and remotely sensed LST datasets. The overall accuracy of the LCZ classification reached an average of 81.7%, which is considered good and acceptable. Mean building fraction, impervious fraction, pervious fraction, SVF, and LST were calculated per LCZ for both cities and compared with value ranges proposed by Stewart and Oke (2012).

Our findings suggest that the sparsely built LCZ (LCZ 9) in a desert environment is difficult to distinguish from bare soil or sand (LCZ F). Moreover, lightweight low-rise LCZ (LCZ 7) and open low-rise LCZ (LCZ 6) exhibit similar surface cover properties, although they have a distinct human activity profile. Properties of heavy industry LCZ (LCZ 10) do not match with proposed value ranges, and SVF values of open high-rise (LCZ 4), open midrise (LCZ 5), and lightweight low-rise (LCZ 7) LCZs are all significantly higher than the LCZ guidelines. Ancillary datasets are necessary to further distinguish between zones in arid desert cities that have a similar spectral signature, and upper boundaries of urban morphological parameters could be adjusted to account for lower height to width ratios in sprawled desert cities.

This study uses remotely sensed LST data derived from TIR satellite images rather than air temperature measurements to perform a LCZ thermal property assessment. It also separates the analysis of daytime LST from nighttime. The LST analysis shows that bare rock or paved (LCZ E) has consistently the highest mean LST among all the LCZ classes during daytime and nighttime for both cities, while water (LCZ G) and low plants (LCZ D) have much lower mean LST. Open high-rise (LCZ 4) exhibits the lowest LST during the daytime among all the built type LCZs, while it shows the highest LST at nighttime for both Phoenix and Las Vegas.

The concept of LCZs is innovative and revolutionary, and many researchers around the world have started exploring and optimizing its knowledge structure in the past few years. Although the LCZ scheme was originally designed to describe distinct local climates delineated by air temperature, our analysis shows that much can be learned from investigating LST in these zones.

We point out that a SUHI analysis of LCZs cannot replace an UHI analysis, because the LST profile of LCZs is different from their air temperature profile, both spatially and temporally. Yet, a complementary analysis of LST signatures for LCZs can give valuable insight into intra-urban LST distributions at the neighborhood scale and facilitate the assessment of urban form impacts on LST.

When investigating arid desert cities or sprawled environments, an adjustment of upper boundaries for aspect ratio and SVF was found to be useful. In the future, more in-depth sensitivity analyses of the automated LCZ classification approach as well as analyses of the results' sensitivity to various parameters (human and physical) are needed in cities of various climate zones and urban morphologies around the world.

Acknowledgements

References

Adams, D.K., Comrie, A.C., 1997. The North American monsoon. Bull. Am. Meteorol. Soc. 78, 2197–2213.

Alexander, P.J., Mills, G., 2014. Local climate classification and Dublin's urban heat island. Atmosphere 5, 755–774.

Anderson, J.R., 1976. A Land Use and Land Cover Classification System for Use with Remote Sensor Data, vol. 964. US Government Printing Office.

Ashie, Y., Ca, V.T., Asaeda, T., 1999. Building canopy model for the analysis of urban climate. J. Wind Eng. Ind. Aerodyn. 81 (1), 237–248.

Balling Jr, R.C., Brazel, S.W., 1987. Time and space characteristics of the Phoenix urban heat island. J. Arizona-Nevada Acad. Sci., 75–81

Bechtel, B., 2011. Multitemporal Landsat data for urban heat island assessment and classification of local climate zones. In: Urban Remote Sensing Event (JURSE), 2011 Joint. IEEE, pp. 129–132.

Bechtel, B., Alexander, P., Böhner, J., Ching, J., Conrad, O., Feddema, J., Mills, G., See, L., Stewart, I., 2015a. Mapping local climate zones for a worldwide database of the form and function of cities. ISPRS Int. J. Geo-Inf. 4, 199–219.

Bechtel, B., Daneke, C., 2012. Classification of local climate zones based on multiple earth observation data. IEEE J. Sel. Top. Appl. Earth Obs. Remote Sens. 5 (4), 1191–1202.

Bechtel, B., Demuzere, M., Sismanidis, P., Fenner, D., Brousse, O., Beck, C., Van Coillie, F., Conrad, O., Keramitsoglou, I., Middel, A., 2017. Quality of crowdsourced data on urban morphology – the human influence experiment (HUMINEX). Urban Sci. 1 (2), 15.

Bechtel, B., Foley, M., Mills, G., Ching, J., See, L., Alexander, P., O'Connor, M., Albuquerque, T., Andrade de, M.F., Brovelli, M., Debashish, D., Fonte, C.C., Petit, G., Hanif, U., Jimenez, J., Lackner, S., Weibo, L., Perera, N., Rosni, N.A., Theeuwes, N., Gál, T., 2015b. CENSUS of cities: LCZ classification of cities (Level 0) – workflow and initial results from various cities. In: 9th International Conference of Urban Climate (ICUC9), Toulouse, France, 20–24 July, 2015, pp. 8–13.

Bechtel, B., See, L., Mills, G., Foley, M., 2016. Classification of local climate zones using SAR and multispectral data in an arid environment. IEEE J. Sel. Appl. Earth Obs. Remote Sens. 9 (7), 3097–3105.

Bouyer, J., Musy, M., Huang, Y., Athamena, K., 2009. Mitigating urban heat island effect by urban design: forms and materials. In: Proceedings of the 5th Urban Research Symposium, Cities and Climate Change: Responding to an Urgent Agenda, Marseille, pp. 28–30.

Ca, V.T., Asaeda, T., Abu, E.M., 1998. Reductions in air conditioning energy caused by a nearby park. Energy Build. 29 (1), 83–92.

Central Arizona-Phoenix Long-Term Ecological Research (CAP LTER), 2015. CAP LTER Land Cover Classification Using 2010 National Agriculture Imagery Program (NAIP) Imagery. Retrieved from <https://sustainability.asu.edu/caplter/data/data-catalog/view/knb-lter-cap.623.1/>.

Danylo, O., See, L., Bechtel, B., Schepaschenko, D., Fritz, S., 2016. Contributing to WUDAPT: a local climate zone classification of two cities in Ukraine. IEEE J. Sel. Top. Appl. Earth Obs. Remote Sens. 9 (5), 1841–1853.

Dyce, D.R., Voogt, J.A., 2018. The influence of tree crowns on urban thermal effective anisotropy. Urban Clim. 23, 91–113.

Fan, C., Myint, S.W., Kaplan, S., Middel, A., Zheng, B., Rahman, A., Huang, H.-P., Brazel, A., Blumberg, D.G., 2017. Understanding the impact of urbanization on surface urban heat islands—a longitudinal analysis of the oasis effect in subtropical desert cities. Remote Sens. 9 (7), 672.

Foody, G.M., 2002. Status of land cover classification accuracy assessment. Remote Sens. Environ. 80 (1), 185–201.

Foody, G.M., 2008. Harshness in image classification accuracy assessment. Int. J. Remote Sens. 29 (11), 3137–3158.

Gál, T., Bechtel, B., Unger, J., 2015. Comparison of two different Local Climate Zone mapping methods. In: 9th International Conference of Urban Climate (ICUC9), Toulouse, France, 20–24 July, 2015.

Geletič, J., Lehnert, M., 2016. GIS-based delineation of local climate zones: the case of medium-sized Central European cities. Mora. Geogr. Rep. 24 (3), 2–12.

Geletič, J., Lehnert, M., Dobrovolný, P., 2016. Land surface temperature differences within Local Climate Zones, based on two central European cities. Remote Sens. 8 (10), 788.

Georgescu, M., Moustaoui, M., Mahalov, A., Dudhia, J., 2011. An alternative explanation of the semiarid urban area "oasis effect". J. Geophys. Res.: Atmos. 116 (D24).

Gillespie, A.R., Rokugawa, S., Hook, S.J., Matsunaga, T., Kahle, A.B., 1999. Temperature/Emissivity Separation Algorithm Theoretical Basis Document (Version 2.4). NASA's Earth Observing System Project Science Office Web Site. Available online at: <http://eospso.nasa.gov/sites/default/files/atbd/atbd-ast-05-08.pdf> (accessed on February 9, 2018).

Hao, X., Li, W., Deng, H., 2016. The oasis effect and summer temperature rise in arid regions-case study in Tarim Basin. Sci. Rep. 6, 35418.

Kong, F., Sun, C., Liu, F., Yin, H., Jiang, F., Pu, Y., Cavan, G., Skelhorn, C., Middel, A., Dronova, I., 2016. Energy saving potential of fragmented green spaces due to their temperature regulating ecosystem services in the summer. Appl. Energy 183, 1428–1440.

Krayenhoff, E.S., Voogt, J.A., 2016. Daytime thermal anisotropy of urban neighbourhoods: morphological causation. Remote Sens. 8, 108.

Leconte, F., Bouyer, J., Claverie, R., Pétrissans, M., 2015. Using Local Climate Zone scheme for UHI assessment: evaluation of the method using mobile measurements. Build. Environ. 83, 39–49.

Lehnert, M., Geletič, J., Husák, J., Vysoudil, M., 2015. Urban field classification by "local climate zones" in a medium-sized Central European city: the case of Olomouc (Czech Republic). Theor. Appl. Climatol. 122 (3–4), 531–541.

Lelovics, E., Unger, J., Gál, T., Gál, C.V., 2014. Design of an urban monitoring network based on Local Climate Zone mapping and temperature pattern modelling. Clim. Res. 60, 51–62.

McCormick, C.M., 1999. Mapping exotic vegetation in the Everglades from large-scale aerial photographs. Photogramm. Eng. Remote Sens. 65 (2), 179–184.

Middel, A., Brazel, A.J., Kaplan, S., Myint, S.W., 2012. Daytime cooling efficiency and diurnal energy balance in Phoenix, AZ. Clim. Res. 54, 21–34.

Middel, A., Häb, K., Brazel, A.J., Martin, C.A., Guhathakurta, S., 2014. Impact of urban form and design on mid-afternoon microclimate in Phoenix Local Climate Zones. Landscape Urban Plann. 122, 16–28.

Middel, A., Lukasczyk, J., Maciejewski, R., 2017. Sky view factors from synthetic fisheye photos for thermal comfort routing—a case study in Phoenix, Arizona. Urban Plann. 2, 19–30.

Middel, A., Lukasczyk, J., Maciejewski, R., 2018. Sky view factor footprints for urban climate modeling. Urban Clim. (in press)

Mills, G., 1999. Urban climatology and urban design. In: Proceedings of the 15th ICB & ICUC, Sydney, Australia, 8–12 November 1999.

Myint, S.W., Wentz, E.A., Brazel, A.J., Quattrochi, D.A., 2013. The impact of distinct anthropogenic and vegetation features on urban warming. Landscape Ecol. 28 (5), 959–978.

Myint, S.W., Zheng, B., Talen, E., Fan, C., Kaplan, S., Middel, A., Smith, M., Huang, H.-P., Brazel, A., 2015. Does the spatial arrangement of urban landscape matter? Examples of urban warming and cooling in Phoenix and Las Vegas. Ecosyst. Health Sustain. 1 (4), 1–15.

NASA LP DAAC, 2001. ASTER Level 2 Surface Temperature Product. Retrieved from <https://doi.org/10.5067/aster/ast_08.003>.

Oke, T.R., 1973. City size and the urban heat island. Atmos. Environ. (1967) 7 (8), 769–779.

Oke, T.R., 1982. The energetic basis of the urban heat island. Quart. J. Roy. Meteorol. Soc. 108 (455), 1–24.

Pearlmutter, D., Krüger, E.L., Berliner, P., 2009. The role of evaporation in the energy balance of an open-air scaled urban surface. Int. J. Climatol. 29 (6), 911–920.

Potchter, O., Goldman, D., Kadish, D., Iluz, D., 2008. The oasis effect in an extremely hot and arid climate: the case of southern Israel. J. Arid Environ. 72 (9), 1721–1733.

Rosenfeld, A.H., Akbari, H., Bretz, S., Fishman, B.L., Kurn, D.M., Sailor, D., Taha, H., 1995. Mitigation of urban heat islands: materials, utility programs, updates. Energy Build. 22 (3), 255–265.

Scepan, J., 1999. Thematic validation of high-resolution global land-cover data sets. Photogramm. Eng. Remote Sens. 65 (9), 1051–1060.

Song, J., Wang, Z.-H., 2015. Impacts of mesic and xeric urban vegetation on outdoor thermal comfort and microclimate in Phoenix, AZ. Build. Environ. 94, 558–568.

Stewart, I.D., Oke, T.R., 2012. Local climate zones for urban temperature studies. Bull. Am. Meteorol. Soc. 93, 1879–1900.

Stewart, I.D., Oke, T.R., Krayenhoff, E.S., 2014. Evaluation of the 'local climate zone' scheme using temperature observations and model simulations. Int. J. Climatol. 34 (4), 1062–1080.

Stewart, J.Q., Whiteman, C.D., Steenburgh, W.J., Bian, X., 2002. A climatological study of thermally driven wind systems of the US Intermountain West. Bull. Am. Meteorol. Soc. 83 (5), 699–708.

Tong, H., Walton, A., Sang, J., Chan, J.C., 2005. Numerical simulation of the urban boundary layer over the complex terrain of Hong Kong. Atmos. Environ. 39 (19), 3549–3563.

Unger, J., Lelovics, E., Gál, T., 2014. Local Climate Zone mapping using GIS methods in Szeged. Hungarian Geogr. Bull. 63 (1), 29–41.

U.S. Climate Data, 2017. Retrieved from: <http://www.usclimatedata.com/>.

Verdonck, M.-L., Okujeni, A., van der Linden, S., Demuzere, M., De Wulf, R., Van Coillie, F., 2017. Influence of neighbourhood information on 'Local Climate Zone' mapping in heterogeneous cities. Int. J. Appl. Earth Observ. Geoinfo. 62, 102–113.

Vinnikov, K.Y., Yu, Y., Goldberg, M.D., Tarpley, D., Romanov, P., Laszlo, I., Chen, M., 2012. Angular anisotropy of satellite observations of land surface temperature. Geophys. Res. Lett. 39.

Vivoni, E.R., Moreno, H.A., Mascaro, G., Rodriguez, J.C., Watts, C.J., Garatuza-Payan, J., Scott, R.L., 2008. Observed relation between evapotranspiration and soil moisture in the North American monsoon region. Geophys. Res. Lett. 35 (22).

Wang, C., Myint, S.W., Wang, Z., Song, J., 2016. Spatio-temporal modeling of the urban heat island in the Phoenix metropolitan area: land use change implications. Remote Sens. 8 (3), 185.

Wulder, M.A., Franklin, S.E., White, J.C., Linke, J., Magnussen, S., 2006. An accuracy assessment framework for large-area land cover classification products derived from medium-resolution satellite data. Int. J. Remote Sens. 27 (4), 663–683.

Yu, C., Hien, W.N., 2006. Thermal benefits of city parks. Energy Buildings 38 (2), 105–120.

Yuan, F., Bauer, M.E., 2007. Comparison of impervious surface area and normalized difference vegetation index as indicators of surface urban heat island effects in Landsat imagery. Remote Sens. Environ. 106 (3), 375–386.

Zheng, Y., Ren, C., Xu, Y., Wang, R., Ho, J., Lau, K., Ng, E., 2017. GIS-based mapping of Local Climate Zone in the high-density city of Hong Kong. Urban Clim. https://doi.org/10.1016/j.uclim.2017.05.008 (in press).